RPE | Radiation Physics & Engineering
A Peer-Reviewed Journal
Published by K.N. Toosi University of Technology
http://rpe.kntu.ac.ir
Research Article

Radiation Physics and Engineering 2024; 5(2):33–41

Evaluation of direct and indirect DNA damage under the photon irradiation in the presence of gold, gadolinium, and silver nanoparticles using Geant4-DNA

Ali Azizi Ganjgah, Payvand Taherparvar*

Department of Physics, Faculty of Science, University of Guilan, Postal Code 4193833697, Rasht, Iran

HIGHLIGHTS

- Effect of the presence different nanoparticles in the vicinity of a DNA is evaluated.
- Gold nanoparticles can cause more DNA damage than gadolinium and silver nanoparticles.
- Increasing the number of nanoparticles results in more DNA damage.

ABSTRACT

Radiation therapy aims to maximize doses to cancer cells while minimizing damage to normal tissues. Today, nanoparticles containing high-atomic-number elements, such as gold, gadolinium, and silver, have proven effective as radiosensitizers in radiotherapy to enhance dose delivery for cancer treatment. In this study, we used the Geant4-DNA toolkit to investigate the effects of multiple nanoparticles (NPs) with varying sizes (radius= 3.15 to 5 nm) on DNA damage when exposed to monoenergetic photons with energies of 15, 40, 50, and 68 keV. Direct and indirect single-strand breaks (SSBs), double-strand breaks (DSBs), and hybrid double-strand breaks (Hybrid DSBs) were calculated in the presence and absence of 1 to 4 nanoparticles (NPs) of the same total volume of gold, gadolinium, and silver nanoparticles for the 1ZBB model (selected from the Protein Data Bank (PDB) library). The results show that increasing the number of gold, gadolinium, and silver NPs and decreasing the photon beam energy increases the total number of strand breaks. Furthermore, gold nanoparticles (GNPs) are more effective options than gadolinium nanoparticles (GdNPs), and silver nanoparticles (SNPs) for inhibiting and controlling cancer cells.

KEYWORDS

DNA damage
Single-strand break
Double-strand break
Hybrid break
Geant4-DNA
Photon beams
Nanoparticle

HISTORY

Received: 16 November 2023
Revised: 28 January 2024
Accepted: 11 February 2024
Published: Spring 2024

1 Introduction

Cancer remains a primary global health concern, responsible for approximately one out of every six deaths worldwide (Debela et al., 2021). Cancer is a complex group of diseases defined by uncontrolled cell growth that progresses through multiple stages. Over time, cells lose the ability to properly regulate their growth and replication (Ganesh and Massague, 2021; Merriel et al., 2021). These days, radiation therapy is used as an effective cancer treatment for over 50% of patients with many types of cancer because it maximizes the radiation dose delivered to cancer cells while minimizing damage to surrounding healthy tissues (Taherparvar and Azizi Ganjgah, 2023; Baskar et al., 2012, 2014). Radiation can be delivered externally using linear accelerators or internally through brachytherapy (Washington and Leaver, 2015). Technological advances have allowed more conformal radiation delivery through techniques like intensity-modulated radiation therapy (IMRT) and image-guided radiation therapy (IGRT) (Mell et al., 2005; Jaffray, 2012). X-rays, gamma rays, electrons, protons, helium, and heavier ions, as well as direct and indirect ionizing rays, are used in radiation therapy to kill tumor cells by specifically targeting them. These rays deposit energy in cells, which excites molecules, especially DNA, leading to irreparable DNA damage and cell death (Yeong et al., 2014; Huynh and Chow, 2021). The energy of these photons' DNA damages both directly and indirectly. They make reactive oxygen species (ROS) and other secondary electrons. The types of DNA damage can usually be grouped into single-

*Corresponding author: p.taherparvar@guilan.ac.ir

https://doi.org/10.22034/rpe.2024.425521.1170

strand breaks (SSBs), and double-strand breaks (DSBs), which are factors that influence the biological effect of exposure to ionizing radiation. While most of these damages can be repaired by DNA repair systems, DSBs are particularly challenging to repair and often result in cell death. Therefore, the DNA within the cell nucleus is considered the primary target for radiation's effects, known as "targeted effects." (Date et al., 2007; Michalik, 1993; Nikjoo et al., 1991; Goodhead, 1994; Ward, 1994; Bedford and Dewey, 2002; Ou et al., 2018). Understanding the mechanisms of DNA damage is essential in fully comprehending the biological nature of radiation sensitivity, making it a suitable criterion for investigating the effects of radiation and ion therapy. Interactions created at the molecular scale are highly complex and cannot be evaluated directly via analytical methods (Thompson, 2012; Ahmadi et al., 2020b). In this way, many reports of Monte Carlo (MC) simulations have been performed as the gold standard for validating radiation dosimetry applications. Today, with the development of the MC codes, radiation transport and distribution of the radiation interactions inside a nucleus, and even more precisely, at the DNA scale can be calculated using MC simulations. It enables to mimic intricate physical and chemical interactions and radiation-induced DNA damage, making more precise predictions of how radiation would affect living cells biologically.

On the other hand, increase the sensitivity of tumor cells to the radiation therapy is very interesting. In this way, radiosensitizers are agents used to improve treatment efficacy (Gong et al., 2021; Siddique and Chow, 2022). They target processes that confer radiation resistance including DNA repair, hypoxia (Fowler et al., 1976), and cell cycle regulation. Major classes of radiosensitizers include oxygen mimetics like the nitroimidazole nimorazole to overcome hypoxia-mediated resistance (Gong et al., 2021); DNA-binding drugs such as cisplatin; molecular inhibitors of oncogenic pathways; and high atomic number nanoparticles that enhance photoelectric interactions. Gold nanoparticles containing high-atomic number elements have a larger absorption cross-section (100 times greater than water), enabling the reduction of radiation doses to normal tissues while increasing dose deposition in cancer cells through heightened photoelectric absorption. This improved tumor-specific energy deposition enhances tumor control (Penninckx et al., 2020; Moore and Chow, 2021).

Numerous research studies have focused on high atomic number nanomaterials like gadolinium (Gd), hafnium (Hf), tantalum (Ta), tungsten (W), and bismuth (Bi) to investigate their potential as radiosensitizers (Rajaee et al., 2019; Fält et al., 2015). Due to their high mass attenuation, these materials exhibit dose enhancement around them when irradiated. However, most of these elements cause damage to healthy tissues when they are in direct contact (Liu et al., 2018; Mardare et al., 2018). Gold nanoparticles (GNPs) are an excellent material for radiosensitization as they provide high-dose enhancement while being biocompatible and avoiding excessive damage to surrounding tissues. GNPs, due to their high atomic number ($Z = 79$) and total absorption cross-section compared to water, about 100 times greater, exhibit a proportionally higher photoelectric absorption cross-section (Shrestha et al., 2016; Chow, 2016b). This interaction between the photons and GNPs increases secondary electron production and enhances dose deposition around the GNPs. Additionally, they have several advantageous properties that make them well-suited for biomedical applications. Their flexibility allows them to be shaped easily and sized precisely, in diameters between 1 to 150 nm (Li et al., 2016). The nanoparticle surface allows the attachment of therapeutic drugs, proteins, or other molecules for targeted delivery (Shrestha et al., 2016; Chen et al., 2020). Gold nanoparticles exhibit low toxicity when administered to patients. Their size distribution is tunable and they also possess unique chemical and optical characteristics beneficial for bioimaging and therapy (Siddique and Chow, 2020; Huang et al., 2012). GNPs are used in radiation therapy to enhance the efficacy of radiation treatments. In addition to utilizing gold nanoparticles, assessing the performance of silver and gadolinium nanoparticles has also received much attention and evaluation (Taha et al., 2019; Hosseini-AliAbadi et al., 2021).

In this study, we extend the investigation of DNA damage in nanoparticle-enhanced radiotherapy presented by Santiago and Chow (Santiago and Chow, 2023), which investigate the effects of 1 to 4 GNPs on DNA damage when irradiated by electron beams different energies. In this way, we used the Geant4-DNA toolkit to investigate the effects of gold nanoparticles (GNPs), gadolinium nanoparticles (GdNPs), and silver nanoparticles (SNPs) with varying sizes (radius= 3.15 to 5 nm) on the SSBs, DSBs, and Hybrid DSBs when exposed to monoenergetic photons with energies of 15, 40, 50, and 68 keV.

2 Materials and Methods

2.1 Monte Carlo Simulation: Geant4-DNA

Various codes have been developed based on the MC method for accurate and reliable prediction of DNA damage. There are two main types of MC codes for simulating radiation transport and DNA damage - Condensed History (CH) and Track Structure (TS) (Ahmadi et al., 2020a; Lazarakis et al., 2018; Kyriakou et al., 2019). CH codes like PENELOPE (Bernal and Liendo, 2009; Baró et al., 1995) and MCNP (Briesmeister, 1986; Titt et al., 2012) simulate the overall macroscopic dose deposition but do not explicitly simulate all interactions at the nanometer scale. They are faster computationally. TS codes like Geant4-DNA (Ganjeh et al., 2021; Salim and Taherparvar, 2022b, 2020, 2022a), PARTRAC (Friedland et al., 2011), and CPA100 (Terrissol and Beaudre, 1990) simulate step-by-step interactions at the molecular/nanometer scale. They are more detailed but computationally intensive. In recent years, among all these codes, the Geant4-DNA code has been widely used in radiobiological applications and nanodosimetry calculations. Geant4-DNA, an extension of Geant4, is one of the most advanced and validated track structure (TS) codes. It is an open-source code written in C++ and works on the cmake platform. It simulates track

structure in liquid water down to the nanometer scale and can model direct and indirect DNA damage. This code can perform structure-pathway simulations at low energies (about eV) to high energy (MeV) with high accuracy (Incerti et al., 2010). It simulates the detailed physical, physicochemical, and chemical processes involved when ionizing radiation tracks traverse liquid water, the main component of biological matter (Lazarakis et al., 2012). Geant4-DNA models interactions down to the nanometer scale by implementing of comprehensive cross-sections for electrons, protons, neutral hydrogen atoms, helium particles, and their respective charged states in liquid water (Incerti et al., 2018). It can simulate track structure and radiation damage at the molecular level, enabling the prediction of diverse DNA damage endpoints like strand breaks, base damage, and clustered damage (Lampe et al., 2018). Applications include micro and nanodosimetry, radiobiology, radiation protection, radiotherapy sensitization with nanoparticles, and space radiation protection (Douglass et al., 2013; Villagrasa et al., 2017). Benchmarking studies have validated Geant4-DNA's accuracy for electrons and light ions (Francis et al., 2011; Nikjoo et al., 1998).

2.2 *Simulation Method and Geometry*

In this research, Geant4-DNA was utilized (Version 11.1.1) to simulate interactions between DNA and photon radiation with energies of 15, 40, 50, and 68 keV (Hsiao et al., 2021; Jabeen and Chow, 2021). The 1ZBB model from the PDBlib (open-source C++ library) was chosen to represent the DNA structure. This model contains 3.1×10^9 base pairs (bp) and mirrors the genome of the African frog, which is frequently used in research due to its similarities with human DNA. The DNA geometry was defined in the "DetectorConstruction" code file. Furthermore, this file was modified by adding 0 (Fig. 1-a), 1 (Fig. 1-b), 2 (Fig. 1-c), and 4 (Fig. 1-d) gold, gadolinium, and silver nanoparticles at distances of 5 nm from the DNA, based on the work of Santiago and Chow. Using Geant4-DNA with a realistic DNA model, we could closely examine how nanoparticle radiation interactions influence the resulting DNA damage patterns. The largest nanoparticle had a radius of 5 nm (a volume of 523.6 nm^3). The parameters used for 2 NPs were a radius of 3.97 nm (a volume of 262.1 nm^3). With both nanoparticles, they would equal about the same as 1 NP. The last parameters used for 4 NPs had a radius of 3.15 nm (a volume of 130.92 nm^3). The total volume of gold, gadolinium, and silver nanoparticles was kept constant at 523.6 nm^3 across all the simulations. The source was defined as mono-energy photons with energies of 15, 40, 50, and 68 keV, located 1 nm from the NPs. The photons were emitted with an isotropic angular distribution. Direct and direct Single-strand break (SSB), Double-strand break (DSB), and Hybrid double-strand break (Hybrid DSB) were calculated in this research. We write code in "EventAction" to calculate SSB, DSB, and Hybrid DSB caused by the physical and chemical stages. An energy threshold of 8.22 eV was utilized for the Physical and Chemical stages (Ganjeh et al., 2021). Indirect damage (chemical stage) produced radicals and molecules, including H_2O_2, H_2, H, H^+, OH^-, OH, and e_{aq-} in water. OH (hydroxyl) has the most significant capacity to interact with DNA (Siddique and Chow, 2022). The hydroxyl radical interacts with sugar and base groups in DNA more than others. The probability of strand break production in DNA by hydroxyl radicals is 13% (P_{OH}= 13%) (Ahmadi et al., 2020b). If the energy deposited in the DNA exceeds the threshold value of 8.22 eV, SSBs will occur. DSB is counted when two SSBs happen on the two strands with a distance of less than 10 base pairs. Hybrid DSB is counted when two SSBs happen (one SSB directly and one SSB indirectly) on the two strands with a distance of less than 10 base pairs (bp). The G4EmDNAPhysics-option6 (Chappuis et al., 2023) and G4EmDNAChemistry-option3 physics lists were applied to simulate the physical and chemical stages, respectively. The Livermore low-energy physics models were used to simulate the interactions between photons and the gold, gadolinium, and silver nanoparticles. To bring the statistical simulation error below 1%, 5×10^8 photons were chosen as the primary particles.

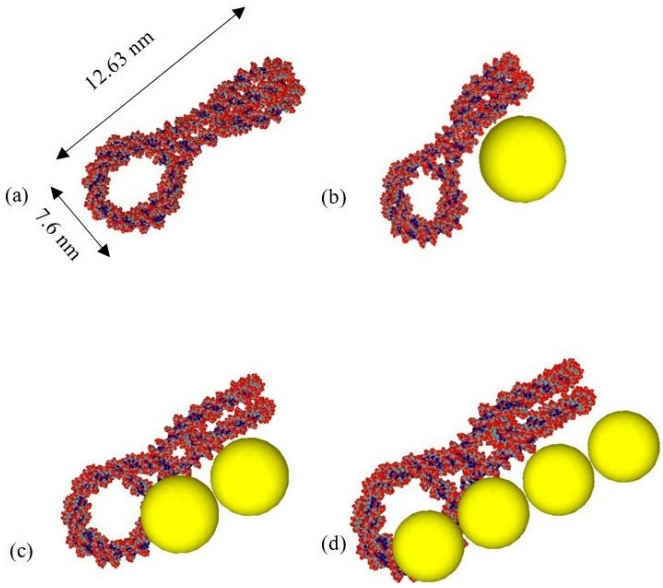

Figure 1: a) OpenGL Visualization of the 1ZBB model. Bases are shown as red spheres, with the first and second strands depicted in blue and gray, respectively. (b) OpenGL Visualization of the 1ZBB and 1 NP with a radius of 5 nm. (c) OpenGL Visualization of the 1ZBB and 2 NPs with a radius of 3.97 nm. (d) OpenGL Visualization of the 1ZBB and 4 NPs with a radius of 3.15 nm.

3 Results and discussion

Figures 2 and 3 show the total number of SSBs and DSBs induced by 15 to 68 keV photons and the influence of gold nanoparticles (GNPs), gadolinium nanoparticles (GdNPs), and silver nanoparticles (SNPs) on the modeled DNA. The number of SSB (DSB) (direct and indirect) in the absence of GNP are 2821 (169), 1369 (74), 789 (44), and 354 (12), for 1GNP are 61573 (3533), 3678 (194),

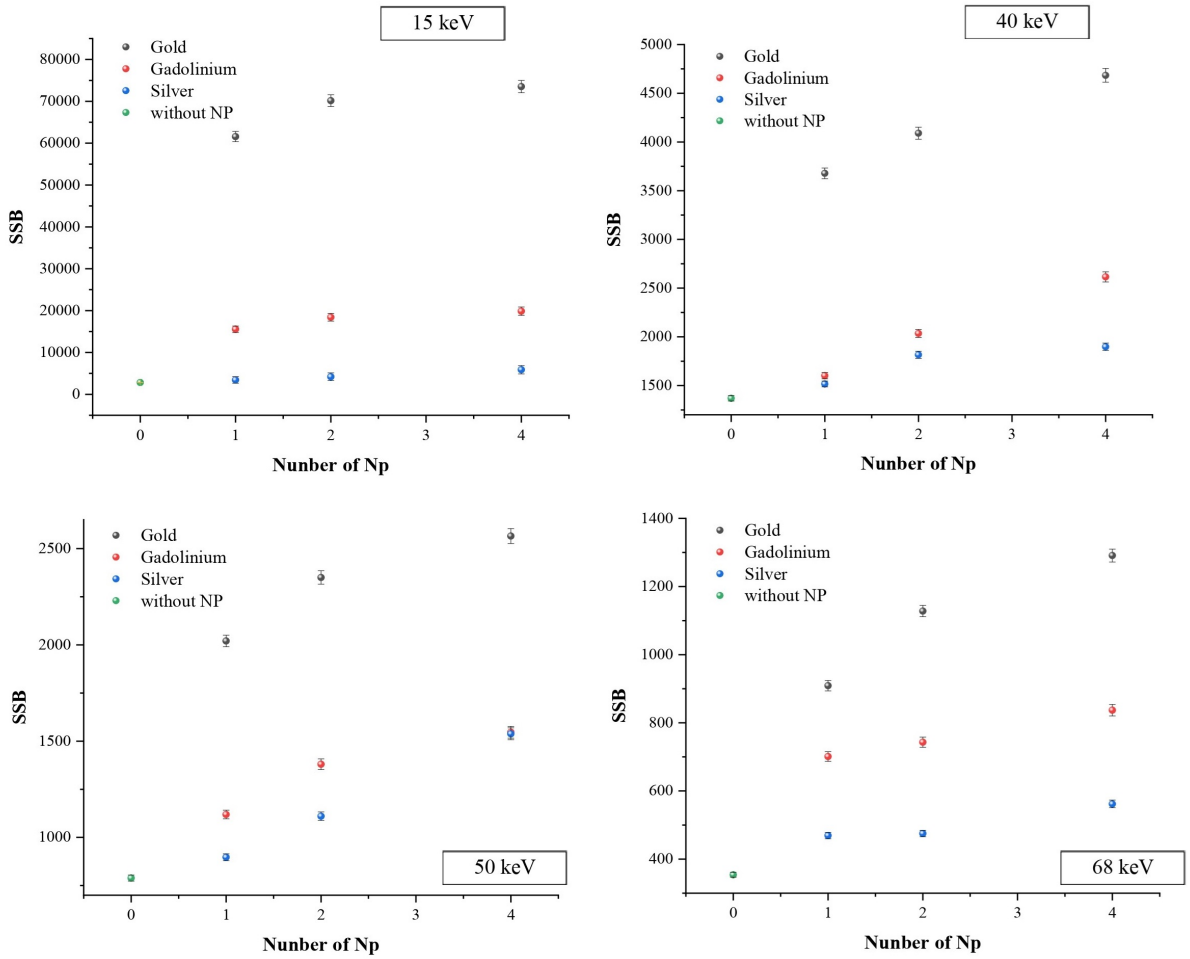

Figure 2: The number of SSBs (direct and indirect) induced by 15, 40, 50, and 68 keV photons for 0, 1, 2, and 4 gold nanoparticles (GNPs), gadolinium nanoparticles (GdNPs), and silver nanoparticles (SNPs).

2020 (97), and 909 (60), for 2GNPs are 70154 (3773), 4090 (228), 2350 (122), and 1128 (78), and for 4GNPs are 73512 (4023), 4684 (235), 2565 (134), and 1291 (90) for the 15, 40, 50, and 68 keV photons, respectively. The addition of 1GNP to the simulated DNA model resulted in an increase in SSB (DSB) (direct and indirect) by 95% (95%), 63% (61%), 61% (54%), and 61% (80%), for 2GNPs 96% (95%), 66% (67%), 66% (64%), and 68% (84%), and 4GNPs 96% (96%), 71% (68%), 69% (67%), and 72% (87%) for the 15, 40, 50, and 68 keV photons, respectively. Also, the number of SSB (DSB) (direct and indirect) for 0GdNP is 2821 (169), 1369 (74), 789 (44), and 354 (12), for 1GdNP are 15546 (890), 1601 (98), 1119 (86), and 701 (39), for 2GdNPs are 18411 (1098), 2035 (111), 1380 (97), and 743 (43), and for 4GdNPs are 19858 (1174), 2615 (183), 1546 (106), and 837 (52) for the 15, 40, 50, and 68 keV photons, respectively. These results for 0SNP are 2821 (169), 1369 (74), 789 (44), and 354 (12), for 1SNP are 3436 (224), 1516 (76), 897 (59), and 469 (30), for 2SNPs are 4208 (257), 1815 (110), 1110 (83), and 475 (39), and for 4SNPs are 5877 (360), 1898 (116), 1538 (88), and 562 (44) for the 15, 40, 50, and 68 keV photons, respectively. The results show adding 1GdNP led to increases in SSB (DSB) (direct and indirect) of 82% (81%), 14% (22%), 29% (49%), and 49% (69%) for the 15, 40, 50, and 68 keV photons, respectively. Also, the addition of 2GdNPs resulted in increases of 85% (85%), 33% (31%), 43% (55%), and 52% (72%), and 4GdNPs led to rises of 86% (85%), 57% (48%), 58% (49%), and 58% (77%) for the 15, 40, 50, and 68 keV photons, respectively. The addition of 1SNP led to increasing 18% (24%), 10% (3%), 12% (25%), and 24% (60%), for 2SNPs 33% (34%), 24% (33%), 29% (47%), and 25% (69%), and 4SNPs 52% (53%), 28% (36%), 49% (50%), and 37% (73%) for the 15, 40, 50, and 68 keV photons, respectively.

The results comparing the nanoparticles show; the increase in SSB (DSB) of GNPs compared to GdNPs for one nanoparticle (1NP) was 75% (75%), 56% (49%), 44% (11%), and 23% (35%), for 2NPs was 74% (71%), 50% (51%), 41% (20%), and 34% (43%), and for 4NPs was 73% (71%), 44% (22%), 40% (21%), and 35% (42%) for the 15, 40, 50, and 68 keV photons, respectively. The results comparing GNPs to SNPs indicate an increase of 94% (94%), 59% (61%), 55% (39%), and 48% (50%) for the 15, 40, 50, and 68 keV photons, respectively in the presence of 1NP. This increase for 2NPs was 94% (93%), 55% (52%), 53% (32%), and 58% (48%), and for 4NPs were 92% (91%), 59% (50%), 40% (34%), and 56% (51%)

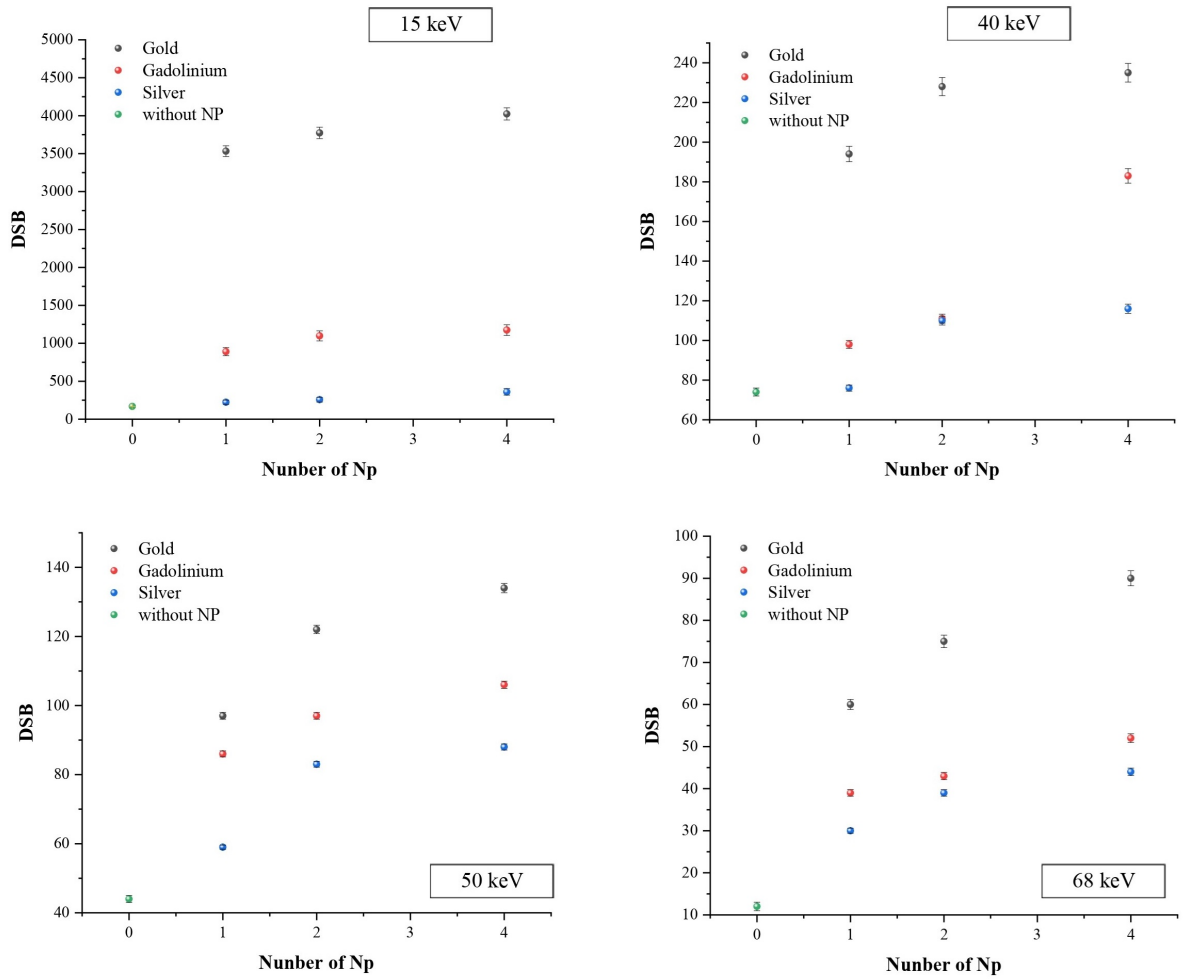

Figure 3: The number of DSBs (direct and indirect) induced by 15, 40, 50, and 68 keV photons for 0, 1, 2, and 4 gold nanoparticles (GNPs), gadolinium nanoparticles (GdNPs), and silver nanoparticles (SNPs).

for the mentioned energies, respectively. Additionally, the results comparing GdNPs to SNPs show an increase of 78% (75%), 5% (22%), 20% (31%), and 33% (23%) for the 15, 40, 50, and 68 keV photons, respectively in the presence of 1NP. This increase for 2NPs was 77% (76%), 11% (1%), 19% (14%), and 36% (9%), and for 4NPs was 70% (69%), 27% (36%), 1% (17%), and 33% (15%) for the mentioned energies, respectively.

Furthermore, Fig. 4 shows the total number of Hybrid DSBs induced by 15-68 keV photons and the influence of GNPs, GdNPs, and SNPs on the DNA. the number of Hybrid DSBs in the absence of gold nanoparticles (GNPs) were 134, 49, 35, and 12 for 15, 40, 50, and 68 keV photons, respectively. With 1 GNP, the numbers were 2613, 142, 89, and 37. With 2 GNPs, the numbers were 2921, 172, 90, and 60. And with 4 GNPs, the numbers were 3130, 178, 110, and 74 for 15, 40, 50, and 68 keV photons, respectively. In addition, in the absence of gadolinium nanoparticles (GdNPs), the numbers were 134, 49, 35, and 12. With 1 GdNP, the numbers were 708, 78, 67, and 36. With 2 GdNPs, the numbers were 830, 84, 71, and 40. And with 4 GdNPs, the numbers were 858, 120, 80, and 58 for 15, 40, 50, and 68 keV photons, respectively. Without silver nanoparticles (SNPs), the numbers were 134, 49, 35, and 12. With 1 SNP, the numbers were 149, 68, 38, and 24. With 2 SNPs, the numbers were 172, 78, 59, and 26. And with 4 SNPs, the numbers were 312, 95, 76, and 37 for 15, 40, 50, and 68 keV photons, respectively.

Moreover, adding 1GNP led to increases in Hybrid DSB of 95%, 65%, 61%, and 67% for the 15, 40, 50, and 68 keV photons, respectively. Also, the addition of 2GNPs resulted in increases of 95%, 72%, 61%, and 80%, and 4GNPs led to rises of 96%, 72%, 68%, and 84% for the 15, 40, 50, and 68 keV photons, respectively. This increase in Hybrid DSB for 1GdNP is 81%, 37%, 48%, and 67%, for 2GdNPs 84%, 42%, 51%, and 70%, and for 4GdNPs 84%, 59%, 56%, and 79% for the 15, 40, 50, and 68 keV photons, respectively. Furthermore, this increase in Hybrid DSB for 1SNP is 10%, 28%, 8%, and 50%, for 2SNPs 22%, 37%, 41%, and 54%, and for 4SNPs 57%, 48%, 54%, and 67% for the 15, 40, 50, and 68 keV photons, respectively. The increase in gold Hybrid DSB compared to gadolinium for 1NP equals 73%, 45%, 25%, and 3%, 2NPs equals 71%, 52%, 21%, and 33% and 4NPs equal to 72%, 32%, 27%, and 21% have been obtained for the 15, 40, 50, and 68 keV photons, respectively. On the other hand, the increase in gold Hybrid DSB compared to silver for 1NP equals 94%, 52%, 57%, and 35%, 2NPs equals 94%, 55%,

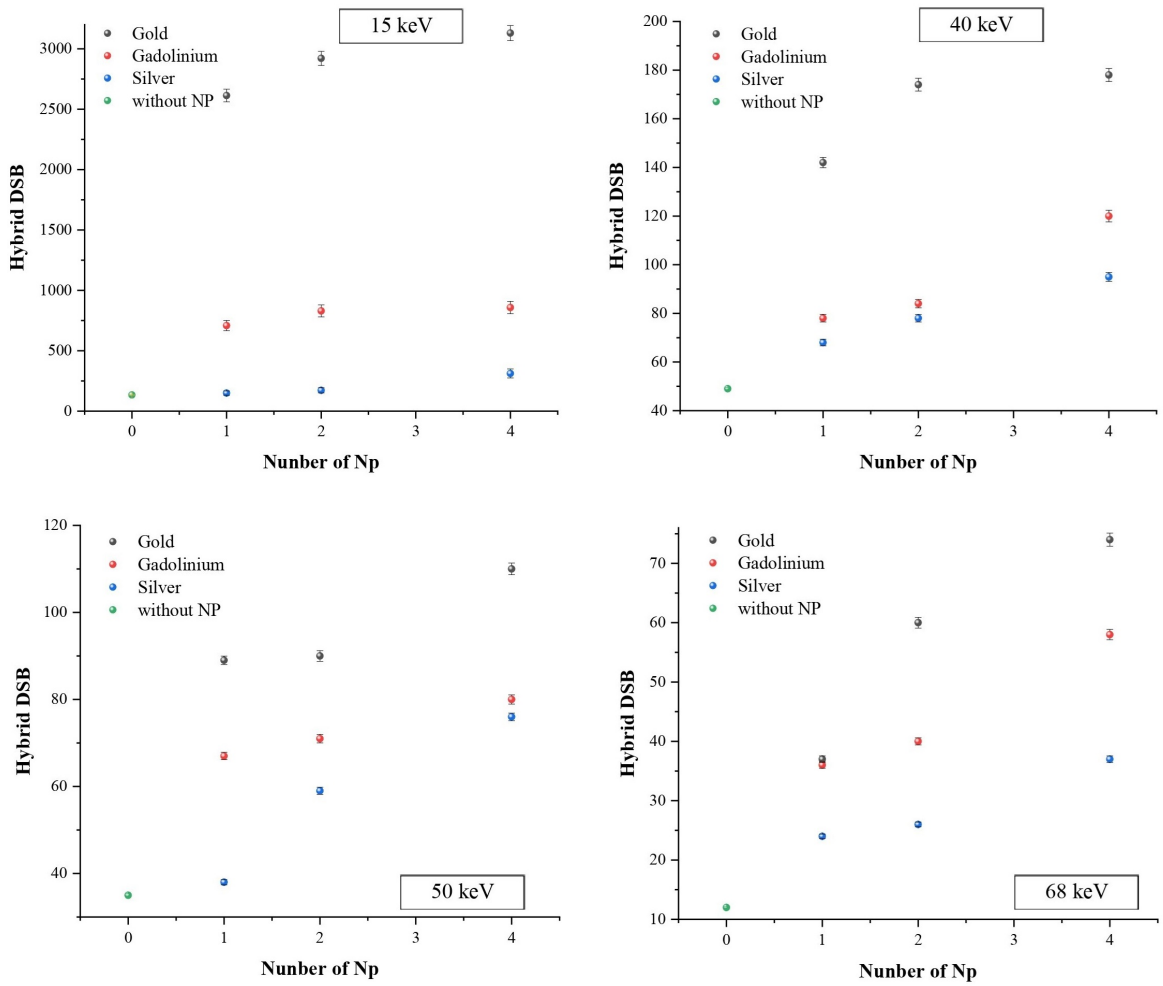

Figure 4: The number of Hybrid DSB induced by 15, 40, 50, and 68 keV photons for 0, 1, 2, and 4 gold nanoparticles (GNPs), gadolinium nanoparticles (GdNPs), and silver nanoparticles (SNPs).

34%, and 57% and 4NPs equal to 90%, 46%, 31%, and 50% have been obtained for the 15, 40, 50, and 68 keV photons, respectively. Also, the increase in gadolinium Hybrid DSB compared to silver for 1NP equals 79%, 13%, 43%, and 33%, 2NPs equals 79%, 7%, 17%, and 35% and 4NPs equal to 63%, 21%, 5%, and 36% have been obtained for the 15, 40, 50, and 68 keV photons, respectively.

Table 1: Table demonstrating the photoelectric interactions when photon beams with energies of 15, 40, 50, and 68 keV irradiated with 1, 2, and 4 GNPs, SNPs, and GdNPs.

		Au	Gd	Ag
Energy	Np	Photoelectric	Photoelectric	Photoelectric
15 keV	1	1.89×10^4	4.29×10^3	2.28×10^3
	2	4.78×10^5	1.11×10^5	6.21×10^4
	4	5.42×10^5	1.25×10^5	7.1×10^4
40 keV	1	1.36×10^3	1.11×10^3	3.9×10^2
	2	3.49×10^4	2.59×10^4	1×10^4
	4	8.2×10^4	3.95×10^4	2.97×10^4
50 keV	1	9.1×10^2	5.8×10^2	2.6×10^2
	2	1.89×10^4	1.44×10^4	7.2×10^3
	4	4.31×10^4	2.2×10^4	1.66×10^4
68 keV	1	2.8×10^2	1.6×10^2	1.1×10^2
	2	8.39×10^3	6.04×10^3	3.83×10^3
	4	1.12×10^4	9.52×10^3	7.03×10^3

The results related to evaluating the SSBs, DSBs, and Hybrid DSBs in the presence of nanoparticles show that GNPs, compared to GdNPs and SNPs in all cases, have caused more DNA breaks. The increased DNA damage caused by GNPs is attributable to gold's high atomic number ($Z = 79$) relative to gadolinium ($Z = 64$) and silver ($Z = 47$). Gold's total absorption cross-section is also about 100 times greater than that of water. On the other hand, Figs. 2 to 4 indicates that the greatest number of strand breaks occurred when 4NPs were added. Increasing the number of NPs from 0 to 4 resulted in a rise in the total number of strand breaks. By holding the volume of Np constant, adding more NPs led to a decrease in the size. This change enhanced the interactions between the NPs and the radiation, therefore increasing the secondary electron yield. These secondary electrons could then be transported to the DNA to cause strand breaks. Another important consideration is the self-absorption of the NP. It was observed that the self-absorption effect became more significant as the NP size increased, leading to a decrease in the secondary electrons produced by the NP and thereby reducing DNA damage. However, in the simulation involving 4 NPs, each NP was smaller than the 1NP. Therefore, the self-absorption effect was less significant,

resulting in the generation of more secondary electrons from the 4 NPs geometry, causing more strand breaks. Furthermore, the presence of a 1NP acted as a "shield", reducing the impact of the secondary electron beams on DNA, thus further decreasing the enhancement of DNA damage.

Moreover, according to Table 1, it can be seen that as the energy of the photon beam decreases, the number of interactions increases. This shows that when low-energy photon beams (15 keV) enter the NP, they lose energy and generate more secondary electrons through photoelectric interaction to enhance number of DNA strand breaks. This can be described by the increase in the photoelectric effect as the cross-section of the photoelectric interaction decreased with higher photon energy. This approach is also recommended by Chow and co-workers (Chow, 2016b,a; Siddique and Chow, 2022; Hsiao et al., 2021). Maximizing DNA damage requires generating the maximum number of secondary electrons through interactions between the incident photons and nanoparticles. However, if the photon energy is too high, the incident photons will likely just penetrate the nanoparticle or undergo limited scattering. This reduces photoelectric interactions and the resultant secondary electron production. To optimize DNA damage, 15 to 68 keV are ideal photon energy range. In this range, photons have enough energy to reach the nanoparticle and produce secondary electrons, but not so much that they pass through the nanoparticle without depositing energy. The results at all stages demonstrated that GNPs have more significant impact on DNA damage, including SSBs, DSBs, and hybrid DSBs, compared to GdNPs and SNPs. This indicates that GNPs can be more effective. The higher atomic number and absorption cross-section of gold allows increased photoelectric interactions and secondary electron production, leading to more extensive DNA damage.

4 Conclusions

In this research, Geant4-DNA was utilized to calculate direct and indirect DNA damage caused by monoenergetic photons with energies of 15-68 keV, both in the absence and presence of gold, gadolinium, and silver nanoparticles. The study established the relationships between photon energy, nanoparticle number, and resulting DNA damage including single-strand breaks (SSBs), double-strand breaks (DSBs), and hybrid DSBs. The 15 keV monoenergetic photons produced the highest and 68 keV monoenergetic photons lowest number of DNA strand breaks, respectively. Our research demonstrated that gold nanoparticles can cause more DNA damage than gadolinium and silver nanoparticles due to gold's high atomic number. The gold nanoparticles increased photoelectric interactions and secondary electron production leading to more significant energy deposition and DNA damage. Specifically, for a given nanoparticle volume, increasing the number of nanoparticles while decreasing their size reduces self-absorption and enables more secondary electron production. This results in enhanced energy deposition in DNA and more DNA damage.

Conflict of Interest

The authors declare no potential conflict of interest regarding the publication of this work.

References

Ahmadi, P., Shamsaei Zafae Ghandi, M., and Shokri, A. (2020a). Calculation of damages of Auger electron emitting from radionuclides based on 1ZBB model: a simulation study using the Geant4 toolkit. *Radiation Safety and Measurement*, 9(6):1–10.

Ahmadi, P., Zafarghandi, M. S., and Shokri, A. (2020b). Calculation of direct and indirect damages of Auger electron-emitting radionuclides based on the atomic geometric model: A simulation study using Geant4-DNA toolkit. *Nuclear Instruments and Methods in Physics Research Section B: Beam Interactions with Materials and Atoms*, 483:22–28.

Baró, J., Sempau, J., Fernández-Varea, J., et al. (1995). Penelope: an algorithm for monte carlo simulation of the penetration and energy loss of electrons and positrons in matter. *Nuclear Instruments and Methods in Physics Research Section B: Beam Interactions with Materials and Atoms*, 100(1):31–46.

Baskar, R., Dai, J., Wenlong, N., et al. (2014). Biological response of cancer cells to radiation treatment. *Frontiers in Molecular Biosciences*, 1:24.

Baskar, R., Lee, K. A., Yeo, R., et al. (2012). Cancer and radiation therapy: current advances and future directions. *International Journal of Medical Sciences*, 9(3):193.

Bedford, J. S. and Dewey, W. C. (2002). Historical and current highlights in radiation biology: has anything important been learned by irradiating cells? *Radiation Research*, 158(3):251–291.

Bernal, M. and Liendo, J. (2009). An investigation on the capabilities of the PENELOPE MC code in nanodosimetry. *Medical Physics*, 36(2):620–625.

Briesmeister, J. F. (1986). MCNP-A general Monte Carlo code for neutron and photon transport. *LA-7396-M*.

Chappuis, F., Tran, H. N., Zein, S. A., et al. (2023). The general-purpose Geant4 Monte Carlo toolkit and its Geant4-DNA extension to investigate mechanisms underlying the FLASH effect in radiotherapy: Current status and challenges. *Physica Medica*, 110:102601.

Chen, Y., Yang, J., Fu, S., et al. (2020). Gold nanoparticles as radiosensitizers in cancer radiotherapy. *International Journal of Nanomedicine*, pages 9407–9430.

Chow, J. C. (2016a). Photon and electron interactions with gold nanoparticles: A Monte Carlo study on gold nanoparticle-enhanced radiotherapy. *Nanobiomaterials in Medical Imaging*, pages 45–70.

Chow, J. C. L. (2016b). Characteristics of secondary electrons from irradiated gold nanoparticle in radiotherapy. In *Handbook of Nanoparticles*, pages 41–65. Springer.

Date, H., Sutherland, K., Hasegawa, H., et al. (2007). Ionization and excitation collision processes of electrons in liquid water. *Nuclear Instruments and Methods in Physics Research Section B: Beam Interactions with Materials and Atoms*, 265(2):515–520.

Debela, D. T., Muzazu, S. G., Heraro, K. D., et al. (2021). New approaches and procedures for cancer treatment: Current perspectives. *SAGE Open Medicine*, 9:20503121211034366.

Douglass, M., Bezak, E., and Penfold, S. (2013). Monte Carlo investigation of the increased radiation deposition due to gold nanoparticles using kilovoltage and megavoltage photons in a 3D randomized cell model. *Medical Physics*, 40(7):071710.

Fält, T., Söderberg, M., Wassélius, J., et al. (2015). Material decomposition in dual-energy computed tomography separates high-Z elements from iodine, identifying potential contrast media tailored for dual contrast medium examinations. *Journal of Computer Assisted Tomography*, 39(6):975–980.

Fowler, J. F., Adams, G. E., and Denekamp, J. (1976). Radiosensitizers of hypoxic cells in solid tumours. *Cancer treatment reviews*, 3(4):227–256.

Francis, Z., Incerti, S., Capra, R., et al. (2011). Molecular scale track structure simulations in liquid water using the Geant4-DNA Monte-Carlo processes. *Applied Radiation and Isotopes*, 69(1):220–226.

Friedland, W., Dingfelder, M., Kundrát, P., et al. (2011). Track structures, DNA targets and radiation effects in the biophysical Monte Carlo simulation code PARTRAC. *Mutation Research/Fundamental and Molecular Mechanisms of Mutagenesis*, 711(1-2):28–40.

Ganesh, K. and Massague, J. (2021). Targeting metastatic cancer. *Nature Medicine*, 27(1):34–44.

Ganjeh, Z. A., Eslami-Kalantari, M., Loushab, M. E., et al. (2021). Calculation of direct DNA damages by a new approach for carbon ions and protons using Geant4-DNA. *Radiation Physics and Chemistry*, 179:109249.

Gong, L., Zhang, Y., Liu, C., et al. (2021). Application of radiosensitizers in cancer radiotherapy. *International Journal of Nanomedicine*, pages 1083–1102.

Goodhead, D. T. (1994). Initial events in the cellular effects of ionizing radiations: clustered damage in DNA. *International Journal of Radiation Biology*, 65(1):7–17.

Hosseini-AliAbadi, S. J., Sardari, D., Saeedzade, E., et al. (2021). Investigation of the extent of DNA damage under proton irradiation in the presence of various nanoparticles of Au, Gd and I, using Geant4-DNA toolkit. *Radiation Safety and Measurement*, 10(2):1–10.

Hsiao, Y.-Y., Tai, F.-C., Chan, C.-C., et al. (2021). A computational method to estimate the effect of gold nanoparticles on X-ray induced dose enhancement and double-strand break yields. *IEEE Access*, 9:62745–62751.

Huang, K., Ma, H., Liu, J., et al. (2012). Size-dependent localization and penetration of ultrasmall gold nanoparticles in cancer cells, multicellular spheroids, and tumors in vivo. *ACS Nano*, 6(5):4483–4493.

Huynh, N. H. and Chow, J. C. (2021). Dna dosimetry with gold nanoparticle irradiated by proton beams: A Monte Carlo study on dose enhancement. *Applied Sciences*, 11(22):10856.

Incerti, S., Ivanchenko, A., Karamitros, M., et al. (2010). Comparison of GEANT4 very low energy cross section models with experimental data in water. *Medical Physics*, 37(9):4692–4708.

Incerti, S., Kyriakou, I., Bernal, M., et al. (2018). Geant4-DNA example applications for track structure simulations in liquid water: a report from the Geant4-DNA Project. *Medical Physics*, 45(8):e722–e739.

Jabeen, M. and Chow, J. C. (2021). Gold nanoparticle DNA damage by photon beam in a magnetic field: A Monte Carlo study. *Nanomaterials*, 11(7):1751.

Jaffray, D. A. (2012). Image-guided radiotherapy: from current concept to future perspectives. *Nature Reviews Clinical Oncology*, 9(12):688–699.

Kyriakou, I., Ivanchenko, V., Sakata, D., et al. (2019). Influence of track structure and condensed history physics models of Geant4 to nanoscale electron transport in liquid water. *Physica Medica*, 58:149–154.

Lampe, N., Karamitros, M., Breton, V., et al. (2018). Mechanistic DNA damage simulations in Geant4-DNA part 1: A parameter study in a simplified geometry. *Physica Medica*, 48:135–145.

Lazarakis, P., Bug, M., Gargioni, E., et al. (2012). Comparison of nanodosimetric parameters of track structure calculated by the Monte Carlo codes Geant4-DNA and PTra. *Physics in Medicine & Biology*, 57(5):1231.

Lazarakis, P., Incerti, S., Ivanchenko, V., et al. (2018). Investigation of track structure and condensed history physics models for applications in radiation dosimetry on a micro and nano scale in Geant4. *Biomedical Physics & Engineering Express*, 4(2):024001.

Li, J., Zhang, J., Wang, X., et al. (2016). Gold nanoparticle size and shape influence on osteogenesis of mesenchymal stem cells. *Nanoscale*, 8(15):7992–8007.

Liu, Y., Zhang, P., Li, F., et al. (2018). Metal-based nanoenhancers for future radiotherapy: radiosensitizing and synergistic effects on tumor cells. *Theranostics*, 8(7):1824.

Mardare, A. I., Mardare, C. C., Kollender, J. P., et al. (2018). Basic properties mapping of anodic oxides in the hafnium–niobium–tantalum ternary system. *Science and Technology of Advanced Materials*, 19(1):554–568.

Mell, L. K., Mehrotra, A. K., and Mundt, A. J. (2005). Intensity-modulated radiation therapy use in the US, 2004. *Cancer: Interdisciplinary International Journal of the American Cancer Society*, 104(6):1296–1303.

Merriel, S. W. D., Ingle, S. M., May, M. T., et al. (2021). Retrospective cohort study evaluating clinical, biochemical and pharmacological prognostic factors for prostate cancer progression using primary care data. *BMJ Open*, 11(2).

Michalik, V. (1993). Estimation of double-strand break quality based on track-structure calculations. *Radiation and Environmental Biophysics*, 32(3):251–258.

Moore, J. A. and Chow, J. C. (2021). Recent progress and applications of gold nanotechnology in medical biophysics using artificial intelligence and mathematical modeling. *Nano Express*, 2(2):022001.

Nikjoo, H., Goodhead, D., Charlton, D., et al. (1991). Energy deposition in small cylindrical targets by monoenergetic electrons. *International Journal of Radiation Biology*, 60(5):739–756.

Nikjoo, H., Uehara, S., Wilson, W., et al. (1998). Track structure in radiation biology: theory and applications. *International Journal of Radiation Biology*, 73(4):355–364.

Ou, H., Zhang, B., and Zhao, S. (2018). Monte Carlo simulation of the relative biological effectiveness and DNA damage from a 400 MeV/u carbon ion beam in water. *Applied Radiation and Isotopes*, 136:1–9.

Penninckx, S., Heuskin, A.-C., Michiels, C., et al. (2020). Gold nanoparticles as a potent radiosensitizer: A transdisciplinary approach from physics to patient. *Cancers*, 12(8):2021.

Rajaee, A., Wang, S., Zhao, L., et al. (2019). Multifunction bismuth gadolinium oxide nanoparticles as radiosensitizer in radiation therapy and imaging. *Physics in Medicine & Biology*, 64(19):195007.

Salim, R. and Taherparvar, P. (2020). Cellular S values in spindle-shaped cells: a dosimetry study on more realistic cell geometries using Geant4-DNA Monte Carlo simulation toolkit. *Annals of Nuclear Medicine*, 34:742–756.

Salim, R. and Taherparvar, P. (2022a). A Monte Carlo study on the effects of a static uniform magnetic field on micro-scale dosimetry of Auger-emitters using Geant4-DNA. *Radiation Physics and Chemistry*, 195:110063.

Salim, R. and Taherparvar, P. (2022b). Dosimetry assessment of theranostic Auger-emitting radionuclides in a micron-sized multicellular cluster model: a Monte Carlo study using Geant4-DNA simulations. *Applied Radiation and Isotopes*, 188:110380.

Santiago, C. A. and Chow, J. C. (2023). Variations in Gold Nanoparticle Size on DNA Damage: A Monte Carlo Study Based on a Multiple-Particle Model Using Electron Beams. *Applied Sciences*, 13(8):4916.

Shrestha, S., Cooper, L. N., Andreev, O. A., et al. (2016). Gold nanoparticles for radiation enhancement in vivo. *Jacobs Journal of Radiation Oncology*, 3(1).

Siddique, S. and Chow, J. C. (2020). Gold nanoparticles for drug delivery and cancer therapy. *Applied Sciences*, 10(11):3824.

Siddique, S. and Chow, J. C. (2022). Recent advances in functionalized nanoparticles in cancer theranostics. *Nanomaterials*, 12(16):2826.

Taha, E., Djouider, F., and Banoqitah, E. (2019). Monte carlo simulation of dose enhancement due to silver nanoparticles implantation in brain tumor brachytherapy using a digital phantom. *Radiation Physics and Chemistry*, 156:15–21.

Taherparvar, P. and Azizi Ganjgah, A. (2023). Effect of marker material on the dosimetric parameters of I-125 source (model 6711): Monte Carlo simulation. *Radiation Physics and Engineering*, 4(2):19–24.

Terrissol, M. and Beaudre, A. (1990). Simulation of space and time evolution of radiolytic species induced by electrons in water. *Radiation Protection Dosimetry*, 31(1-4):175–177.

Thompson, L. H. (2012). Recognition, signaling, and repair of DNA double-strand breaks produced by ionizing radiation in mammalian cells: the molecular choreography. *Mutation Research/Reviews in Mutation Research*, 751(2):158–246.

Titt, U., Bednarz, B., and Paganetti, H. (2012). Comparison of MCNPX and Geant4 proton energy deposition predictions for clinical use. *Physics in Medicine & Biology*, 57(20):6381.

Villagrasa, C., Meylan, S., Gonon, G., et al. (2017). Geant4-DNA simulation of dna damage caused by direct and indirect radiation effects and comparison with biological data. In *EPJ web of Conferences*, volume 153, page 04019. EDP Sciences.

Ward, J. (1994). The complexity of DNA damage: relevance to biological consequences. *International Journal of Radiation Biology*, 66(5):427–432.

Washington, C. M. and Leaver, D. T. (2015). *Principles and practice of radiation therapy-e-book*. Elsevier Health Sciences.

Yeong, C.-H., Cheng, M.-h., and Ng, K.-H. (2014). Therapeutic radionuclides in nuclear medicine: current and future prospects. *Journal of Zhejiang University. Science. B*, 15(10):845.

To cite this article:

Azizi Ganjgah, A., Taherparvar, P. (2024). Evaluation of direct and indirect DNA Damage under the Photon Irradiation in the Presence of Gold, Gadolinium, and Silver Nanoparticles Using Geant4-DNA. *Radiation Physics and Engineering*, 5(2), 33-41.

DOI: 10.22034/rpe.2024.425521.1170

To link to this article: https://doi.org/10.22034/rpe.2024.425521.1170